Optimum Jet Mixing in a Tubular Reactor

Larry J. Forney and Noureddine Nafia
School of Chemical Engineering, Georgia Institute of Technology, Atlanta, GA 30332

Hanh X. Vo
Dow Corning Corp., Midland, MI 48686

The rapid mixing of two miscible fluids is a precursor to promoting fluid-phase reactions. The configuration of a turbulent jet in a crossflow or tee-mixer is the most efficient passive design for rapid mixing. Here the Damkohler number has been defined from available tee-mixer data where the reactions are slow to fast compared with mixing times. For the available data the Damkohler number has been found to be of secondary importance for optimum design. The numerical simulation of jets in a tubular reactor suggests that large jet-to-tube momentum ratios with no backmixing are superior. Moreover, the optimum design of maximum jet entrainment is shown to be synonymous with either a minimum in the relative standard deviation or the skewness. A formula relating the optimum diameter ratio to the jet-to-tube flow ratio has also been derived assuming geometrically similar jet trajectories, and the result correlates both numerical and experimental data.

Introduction

Turbulence promotes most important chemical reactions, heat-transfer operations, mixing, and combustion processes in industry. Effective use of turbulence increases reactant contact and decreases reaction times, which can significantly reduce the cost of producing many chemicals. Efficient mixing is necessary to obtain profitable yields in mixing operations that can be generally classified as either distributive or phase dispersive.

It is common in many existing chemical process units to continuously mix two fluids in a tubular reactor. If the Reynolds number $Re > 2{,}000$, the flow is turbulent and mixing results from turbulent diffusion. Since all mixing applications require the injection of fluid into the reactor at one or more locations, a mixing tee as shown in Figure 1 provides a simple method of contacting two fluid streams. In fact, it is possible to achieve variation coefficients $\sigma/\bar{x} < 0.05$ that are suitable for many industrial applications in less than 10 tube diameters from the injection point (Sroka and Forney, 1989; Forney and Gray, 1990; Monclova and Forney, 1995). Moreover, for fast reaction applications that require short residence times, a tee-mixer is an attractive alternative to stirred tanks. The former is easier to scale up and represents a more economical, reproducible and efficient design for rapid mixing.

Examples of specific applications for tee mixers are low-viscosity fluid mixing such as the dilution of concentrated acids or bases, wastewater treatment, or blending petrochemical products. Other important commercial blending examples are injecting a supersaturated steam into a crystallizer, or injecting a feed stream containing either a catalyst or monomer in polymerization reactors (Bourne, 1992). The quality of mixing also strongly influences the product distribution resulting from fast competitive reactions (Bourne et al., 1982). Examples of the latter are either the production of

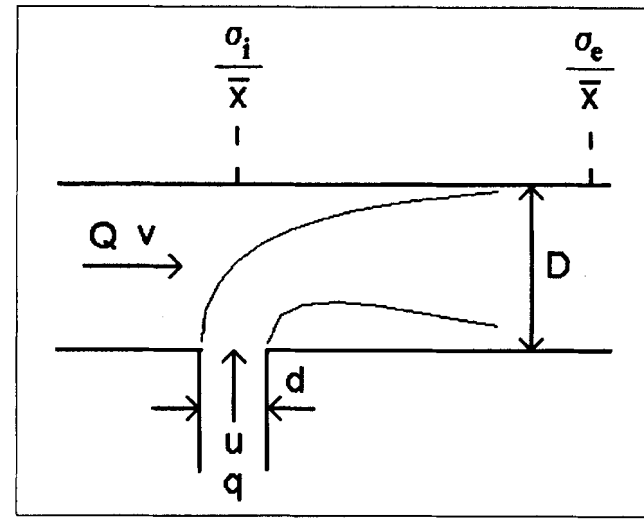

Figure 1. Mixing tee.

silicone or polyolefin plastics (Ver Strate et al., 1988; Cozewith et al., 1991). Gas mixing applications are the blending of fuel gases, mixing of feed streams for catalytic reactors, where $\sigma/\bar{x} < 10^{-3}$, and mixing hot flue gases with ambient air. Important industrial examples of gas mixing are the chlorination of gaseous hydrocarbons, oxidation of ethylene, and the air oxidation of ammonia (Ajinkya, 1983). Additional information is available in the reviews of mixing with tees prepared by Simpson (1974), Gray (1986), and Forney (1986).

The first systematic study of tee mixing by jet injection was conducted by Chilton and Genereaux (1930), who used smoke visualization techniques to determine optimum mixing conditions at a glass tee. They concluded that right-angle configurations were effective for good mixing. Chilton and Genereaux also found that when the ratio of the velocity of secondary-to-main flow was in the range of 2–3, satisfactory mixing was obtained in 2–3 tube diameters. Narayan (1971) and Reed and Narayan (1979) used quantitative methods to measure the degree of mixing of air–carbon dioxide feed streams in three pipeline mixers. Narayan, like Chilton and Genereaux, found it was possible to achieve rapid mixing in a few tube diameters with perpendicular jet injection devices or tee mixers, but that parallel or coaxial flow geometries required up to 250 tube diameters (see the Appendix).

More recently, several detailed experiments have been conducted characterizing jet injection of fluid by a mixing tee near the injection point (less than 12 tube diameters). Forney and Kwon (1979) and Forney and Lee (1982) established the importance of the diameter and velocity ratio for geometrically similar flows. O'Leary and Forney (1985) indicated the importance of the Reynold's and Froude numbers. Maruyama et al. (1981, 1982, 1983) related mixing quality to the standard deviation and provided limited data for optimum conditions. Gosman and Simitovic (1986) indicated that wall impaction may improve the mixing quality with inert components. Finally, Sroka and Forney (1989) developed a similarity law relating the variation coefficient with the jet-to-tube momentum ratio and distance from the injection point. Ger and Holley (1976) and Fitzgerald and Holley (1981) compared standard deviations of measured tracer concentrations far downstream (7–120 tube diameters) from the side tee.

Tee-mixer design has been shown to strongly influence either the reaction rate for fast simple reactions or product distribution resulting from fast competing reactions. Tosun (1987) measured the selectivity of coupled reactions and clearly demonstrated an optimum velocity ratio for three jet-to-tube diameter ratios. For a fixed diameter ratio, however, measurements of selectivity were averaged for several values of a small Damkohler number. Thus, it was difficult to determine the influence of mixing-to-reaction time on the yield when both times were of the same order. Cozewith and Busko (1989) measured the indicator color length in an HCl/NaOH neutralization reactor. Cozewith and Busko also found an optimum velocity ratio for a given tee geometry in the mixing controlled limit of very large Damkohler numbers. Cozewith et al. (1991) also attempted to show for a polymerization reaction that the narrowest copolymer composition at one diameter ratio occurred at the same conditions that optimized mixing in the absence of reaction.

In the present article the optimum tee-mixer designs from the experimental reaction data of both Tosum (1987) and Cozewith and Busko (1989) are compared where the reactions are slow to fast compared to mixing times. In this context, the Damkohler number has been introduced into the correlation and discussed. Results from complete numerical computations (PHOENICS version 2.1) of the relative standard deviation, skewness, and jet entrainment rates are found to be analogous and are favorably compared with the reaction data. A scaling law is also derived by assuming that optimum mixing corresponds to a geometrically similar jet trajectory.

Jet Injection in Tubular Reactors

The rapid mixing of two fluids of the same phase is a precursor to carrying out fluid-phase reactions. The configuration of a turbulent jet in a crossflow is the most effective passive design for rapid mixing. In the tee mixer shown in Figure 1, the characteristic mixing time defined as the ratio of jet diameter-to-velocity, d/u, can be as small as 10^{-4} s. In general, increasing the rate of entrainment of ambient tube fluid into the jet decreases the mixing time and improves the reactor yield.

Dimensional analysis

A dimensional analysis of right-angle jet injection into a tubular reactor as shown in Figure 1 suggests a conversion ratio

$$X_s = f\left(\frac{d}{D}, \frac{u}{v}, Re_j, Da, x/D\right), \tag{1}$$

where X_s may represent the yield from a simple reaction or the selectivity from a competing reaction scheme. Equation 1 is restricted to a given reaction with constant stoichiometry (i.e., molar flow-rate ratios of reactants are constant). In Eq. 1, Re_j $(= du/\nu)$ is the jet Reynolds number and Da is the Damkohler number defined as the ratio of mixing-to-reaction time

$$Da = \frac{kx_j d}{u}, \tag{2}$$

where x_j is the initial concentration of the jet reactant and k is the rate constant (see Appendix 2).

In the present article the reaction times are assumed to be small compared to the characteristic mixing times for either simple reactions or reactions producing desirable products in a competitive scheme. It is therefore assumed that these reactions are complete within the first two tube diameters from the jet injection point since the mixing time is much less than the flow time $(d/u \ll D/v)$ or that the quality of mixing can be evaluated at fixed $x/D = 2.0$. We also assume that the quality of mixing is independent of the jet Reynolds number, provided $Re_j > 9 \times 10^3$ (Forney and Kwon, 1979). Maximizing the yield X_s in Eq. 1 by setting $\partial X_s/\partial(u/v) = 0$ provides a unique relationship between diameter and velocity ratio (or flow ratio). Thus, an optimum geometry for jet mixing can be written in the form

$$\frac{d}{D} = f(q/Q, Da), \tag{3}$$

where for convenience the mixing ratio $q/Q = (u/v)\,(d/D)^2$.

Numerical computations

The general-purpose computational fluid dynamic (CFD) code available in the PHOENICS package was used to solve finite-volume equivalent expressions for the basic conservation equations of mass, momentum, and species concentration. The k-ϵ turbulent model provided concentrations on a computational grid limited to one half the tube cross-sectional area because of symmetry for two tube diameters in length from the fluid injection point. The grid consisted of $15 \times 20 \times 68$ points in the radial, azimuthal, and axial coordinates, respectively, with an additional tube diameter upstream from the injection point. The details of the computation including a description of the standard wall functions and sensitivity to empirical constants in the turbulent model are discussed in an earlier article (Monclova and Forney, 1995).

The flow in the tee mixer was modeled as a steady turbulent flow of a single-phase fluid containing an inert tracer introduced at the injection point with volume ratio $x_j = 0.2$. Figure 2 illustrates concentration contours for a tee mixer with excess jet momentum. The jet projects across the tube, impacts with the opposite wall, and creates a region of backmixing. This configuration does not provide maximum jet entrainment at the inlet nor optimum conditions defined by the yield from fast reactions. Most of the mixing occurs after the jet impacts with the opposite wall. At the bottom of Figure 2 are concentration profiles across the tube at $x/D = 2.0$ downstream from the injection point. As expected, the concentration distribution is asymmetric with regions of high concentrations near the opposite wall of the tube.

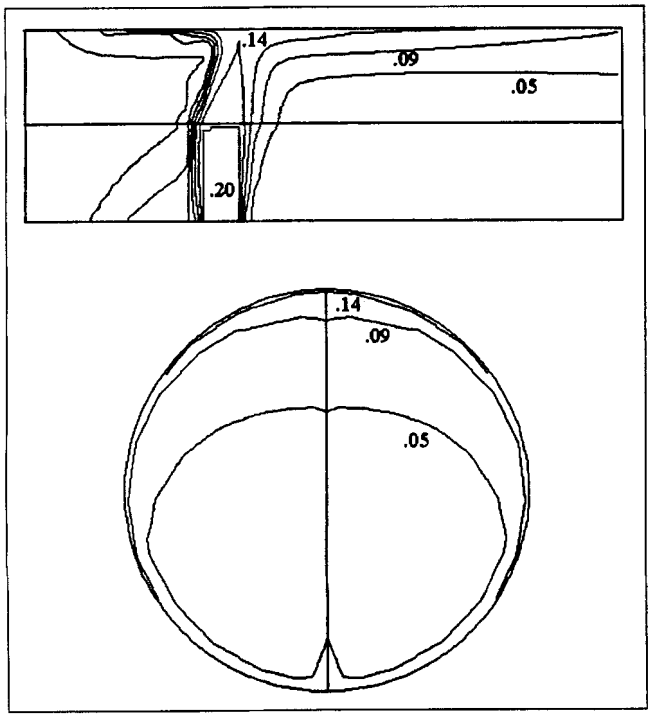

Figure 2. Concentration profiles with excess jet momentum; $d/D = 0.2$, $u/v = 9.0$.

In the top, the flow is left to right and numbers are tracer concentrations (volume fraction). Bottom is tube cross section downstream from jet inlet; $x/D = 2.0$.

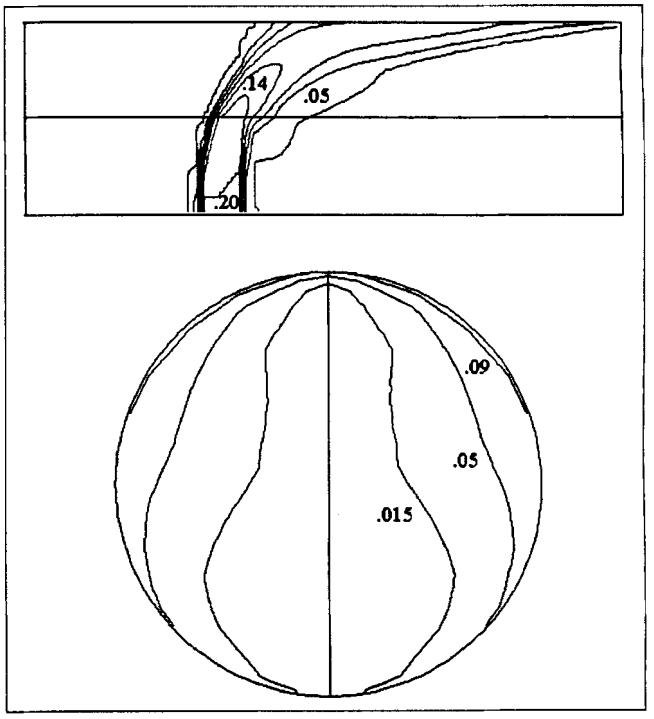

Figure 3. Concentration profiles with optimum jet momentum; $d/D = 0.2$, $u/v = 4.0$.

Bottom is tube cross section downstream from jet inlet; $x/D = 2.0$.

Figure 3 illustrates the flow pattern for optimum conditions of maximum jet entrainment and yield from fast reactions. The mixing quality defined in terms of optimum properties of the concentration profile (e.g., relative standard deviation) at a tube cross section at $x/D = 2.0$ is compared with experimental geometries for optimum mixing with fast reactions later. The configuration of jet impingement against the opposite wall for optimum mixing near the jet inlet is consistent with the measurements of Maruyama et al. (1981), Gosman and Simitovic (1986), and Cozewith and Busko (1989). At the bottom of Figure 3 are the concentration profiles at $x/D = 2.0$ that demonstrate symmetry between the near and far wall (bottom and top) of the tubular reactor.

Statistics of Jet Mixing

In the present article an inert tracer of volume ratio $x_j = 0.2$ was injected by the side stream in Figure 1. The numerical computations provide concentration values across the grid. Uniformity criteria were defined in terms of the second and third moments about the arithmetic mean $\bar{x}$ at a given tube cross-sectional area at two diameters downstream from the injection point $x/D = 2.0$.

Second moment

The second moment about the mean $\bar{x}$ is defined for a given tube cross section A in the form

$$m_2 = \int_A (x - \bar{x})^2 u \, dA / \int_A u \, dA, \tag{4}$$

where the total volumetric flow rate

$$\int_A u\,dA = q + Q.$$

Here, q, Q are the jet and main stream volume flow rates in Figure 1, respectively, and u is the fluid velocity parallel to the tube axis. The quantity x in Eq. 4 represents either a concentration or volume fraction.

The arithmetic mean of the concentration $\bar{x}$ in Eq. 4 is defined for a given tube cross-sectional area A in the form

$$\bar{x} = \int_A xu\,dA / \int_A u\,dA, \tag{5}$$

or, more conveniently, in terms of the uniform inlet conditions

$$\bar{x} = \frac{x_j q}{q + Q}. \tag{6}$$

A number of common expressions for uniformity are defined in terms of $m_2 = \sigma^2$ the variance and the mean $\bar{x}$. The variation coefficient defined as the dimensionless ratio of standard deviation to the mean $\bar{x}$ can be written in the form

$$\frac{\sigma_e}{\bar{x}} = \left(\frac{\sigma_i}{\bar{x}}\right)\left(\frac{\sigma_e}{\sigma_i}\right), \tag{7}$$

where $\sigma_e/\bar{x}$ is the exit variation coefficient, $\sigma_i/\bar{x}$ is the initial value at the jet inlet, and σ_e/σ_i is the relative standard deviation as shown in Figure 1.

The variation coefficient $\sigma/\bar{x}$ is a measure of the local stream concentration uniformity while the relative standard deviation σ_e/σ_i is a measure of the mixer performance. The latter would be influenced by the mixer geometry, fluid Reynolds number, and flow rates. In the present case

$$\frac{\sigma_e}{\sigma_i} = f(u/v,\ d/D,\ x/D) \tag{8}$$

for sufficiently large jet Reynolds number. If x/D is fixed and one seeks a minimum in σ_e/σ_i, or setting $\partial(\sigma_e/\sigma_i)/\partial(u/v) = 0$, the geometry is predicted in the form

$$\frac{d}{D} = f(q/Q) \tag{9}$$

similar to Eq. 3 in the absence of chemical reactions.

Numerical computations of the exit variation coefficient $\sigma/\bar{x}$ for fixed tee-mixer geometry are shown in Figure 4. As indicated, the value of $\sigma_e/\bar{x}$ decreases with increasing jet-to-tube momentum ratio $(l_m/D)^2 = (u/v)^2\,(d/D)^2$. Although the optimum momentum ratio for maximum yield from fast reactions occurs within the indicated range, it would be difficult to choose its value.

However, numerical results of the relative standard deviation shown in Figure 5 indicate clues for choosing the optimum velocity ratio. As the momentum ratio increases, the

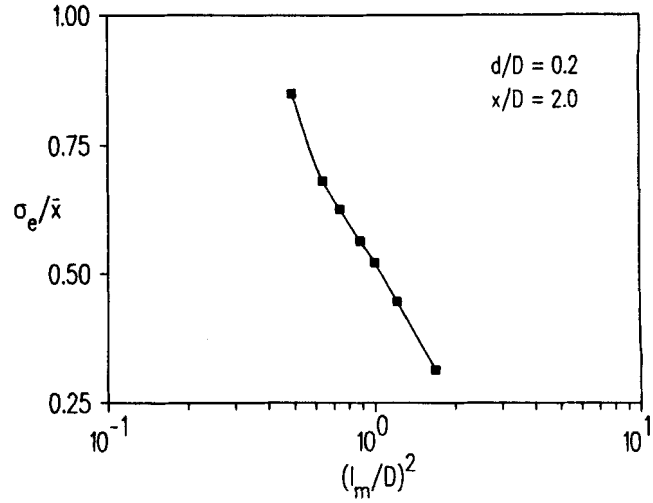

Figure 4. Variation coefficient vs. jet-to-tube momentum ratio for fixed mixing-tee dimensions.

relative standard deviation decreases until $(l_m/D)^2 = 0.63$. The decrease in σ_e/σ_i results from increasing jet entrainment near the jet inlet. For values of $(l_m/D)^2 > 0.63$, the dominant mechanism for mixing shifts from jet entrainment to wall impaction. Although the mixer performance in the latter case is enhanced at large momentum ratios, the contacting between reactants occurs away from the jet inlet and the yield from fast reactions is less than optimum.

As discussed later, the optimum velocity ratio for fast reactions is determined from the local minimum in the value of the relative standard deviation σ_e/σ_i at $(l_m/D)^2 = 0.63$ or $u/v \cong 4.0$ where the jet entrainment rate is a maximum. Plots of the type indicated in Figure 5 provide a relationship between optimum diameter ratio d/D and velocity u/v or flow ratio q/Q as suggested by Eq. 9.

Initial variation coefficient

Values of relative standard deviation plotted in Figure 5 were computed from the ratio of exit-to-inlet variation coeffi-

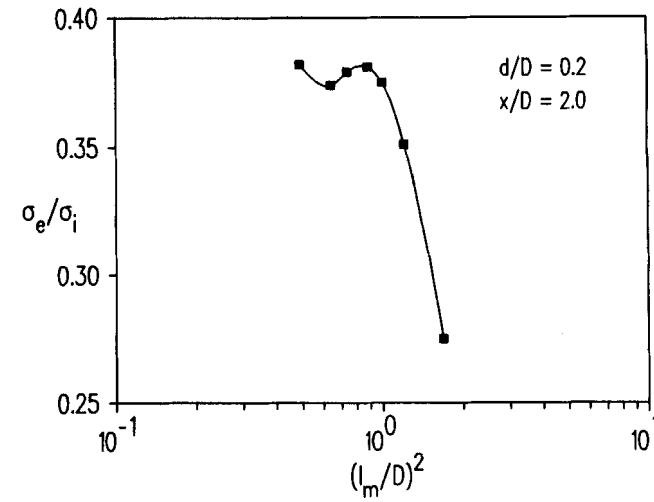

Figure 5. Relative standard deviation vs. jet-to-tube momentum ratio for fixed mixing-tee geometry.

cient defined by Eq. 7. The initial variation coefficient is an analytic expression derived from Eq. 4 where the area A is the total of the tube cross section and jet inlet. Since $m_2 = \sigma^2$, one obtains

$$\sigma_i^2 = \frac{1}{q+Q}\left[(x_j - \bar{x})^2 q + \bar{x}^2 Q\right] \tag{10}$$

because the volume fraction of the tracer $x = 0$ in the tube upstream from the jet inlet. Dividing Eq. 10 by $\bar{x}^2$ and rearranging, one obtains (Gray, 1986)

$$\frac{\sigma_i}{\bar{x}} = \left(\frac{x_j - \bar{x}}{\bar{x}}\right)^{1/2} = \left(\frac{Q}{q}\right)^{1/2}. \tag{11}$$

For the simple geometry of turbulent flow in a cylindrical tube or pipe, Eq. 4 can be simplified by setting $u = 1$. This has little effect on values of the second moment m_2 downstream, and the initial variation coefficient is computed in the form (Maruyama et al., 1983)

$$\frac{\sigma_i}{\bar{x}} = \left[\frac{(d/D)^2(Q/q)^2 + 1}{(d/D)^2 + 1}\right]^{1/2}. \tag{12}$$

Equation 12 was used to compute the numerical values of σ_e/σ_i in Figure 5.

Third moment

Another measure of concentration uniformity is the degree of asymmetry, or departure from symmetry, of a distribution. For example, if the distribution of tracer is concentrated in one area off the center, the distribution is said to be skewed. An important measure of skewness uses the third moment about the mean expressed in dimensionless form $m_3/m_2^{3/2}$, where the degree of skewness has been normalized by the standard deviation of the distribution. Here,

$$m_3 = \int_A (x - \bar{x})^3 u\, dA / \int_A u\, dA. \tag{13}$$

The value of $m_3/m_2^{3/2}$ is called the moment coefficient of skewness where m_2 is defined in Eq. 4 and A is the tube cross-sectional area.

Effects of turbulent model

The turbulent model used in the numerical computations, in particular the wall function, can influence the computed concentration distribution and thus moments used to define uniformity. The problem is important when the jet momentum is large and wall impaction is important.

The relative standard deviation σ_e/σ_i was computed with three wall functions: low Re, two-layer k-ϵ, and the standard wall function used with the k-ϵ model. These results are presented in Figure 6. As expected, there are differences between the predictions of the three models at large jet-to-tube momentum ratios $(l_m/D)^2 > 1.0$. However, maximum jet entrainment rates that provide the optimum geometry for applications to fast reactions occur at the local minimum of σ_e/σ_i at $(l_m/D)^2 \cong 0.45$, where the three models provide identical results. As a result, the k-ϵ turbulent model with the standard wall function was used in the present study as described elsewhere (Monclova and Forney, 1995).

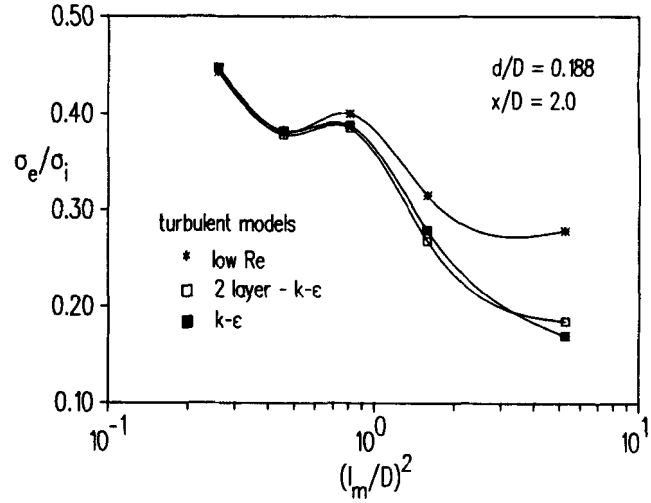

Figure 6. Relative standard deviation vs. jet-to-tube momentum ratio for three turbulent models.

Results and Discussion

Existing experimental data are compared with the numerical computations of tracer concentration moments in addition to results from the concepts of maximum jet entrainment and geometric similarity.

Fast reaction data

When two streams are fed to a tubular reactor the segregation of the reactants will affect the reactor performance (Brodkey, 1975; Toor, 1975; Patterson, 1975). For simple reactions, poor mixing will reduce the yield, but for competing reactions the product composition will exhibit dramatic differences depending on the mixer performance. For the case of jet injection into a tubular reactor, good mixing always means greater entrainment of ambient fluid into the jet near the jet inlet.

Tosun (1987) studied the performance of a tee mixer with the competitive–consecutive reaction scheme described by Bourne et al. (1981)

$$A + B \xrightarrow{k_1} R$$
$$R + B \xrightarrow{k_2} S. \tag{14}$$

The purpose of these experiments was to determine the optimum geometry that maximized the yield of component R (minimize S). Tosun determined the optimum velocity ratio u/v that minimized S for three jet-to-tube diameter ratios as tabulated in Table 1. For fixed molar flow rates of A (tube) and the limiting reactant B (jet), the fractional conversion of B to S or $X_s \cong 0.10$ for the data in Table 1. These data correspond to the maximum entrainment of A into the jet containing B, which reduces the segregation of the reactants, the

Table 1. Optimum Geometry for Fast Reactions

Tosun (1987), $k_1 = 7.3\times10^3$ m^3·mol^{-1}·s^{-1}; $k_2 = 3.5$ m^3·mol^{-1}·s^{-1}; $x_j = 0.98$ mol/m^3

				Damkohler No.	
d/D	u/v	d (cm)	u (m/s)	k_1x_jd/u	k_2x_jd/u
0.085	11.8	0.9	28.4	2.3	1.1×10^{-3}
0.125	6.8	0.9	27.3	2.3	1.1×10^{-3}
0.25	3.0	1.8	7.4	17.3	0.83×10^{-2}

Cozewith and Busko (1989), $k = 10^8$ m^3·mol^{-1}·s^{-1}; $x_j \cong 1$ mol/m^3

d/D	u/v	d (cm)	u (m/s)	kx_jd/u
0.047	9.0	0.12	13.4	0.9×10^4
0.078	7.1	0.2	13.2	1.5×10^4
0.125	5.4	0.32	9.8	3.3×10^4
0.188	3.6	0.48	7.0	6.9×10^4
0.250	3.1	0.64	6.0	1.1×10^5

local concentration of B near the inlet, and the rate of formation of S by the competing reaction of Eq. 14.

The Damkohler numbers computed for the Tosun data in Table 1 are calculated with the small rate constant $k_2 = 3.5$ m^3·mol^{-1}·s^{-1} for the second reaction of Eq. 14. The small Da numbers in the range of 10^{-3} to 10^{-2} for the second reaction indicate that these reaction times are large relative to the mixing times, which is supported by the measured selectivity $X_s \cong 0.10$ near the kinetic limit or minimum $X_s = 0.002$ (in contrast, $X_s \to 1.0$ for $Da \gg 1$). Baldyga and Bourne (1989) and Bourne and Yu (1994) demonstrated that X_s varied over a range of $10^{-3} < Da < 10^3$ with an engulfment model applied to a semibatch reactor. These results are consistent with the magnitude of $Da \cong 10^{-3}$ computed for the small values of $X_s \cong 0.1$ near the kinetic limit as measured by Tosun.

Cozewith and Busko (1989) measured tee performance by observing the reaction zone or distance to mix with a fast simple reaction for the neutralization of NaOH in the tee with HCl in the main stream.

$$\mathrm{NaOH} + \mathrm{HCl} \xrightarrow{k} \mathrm{NaCl} + \mathrm{H_2O}. \qquad (15)$$

In these experiments the optimum velocity ratio u/v was recorded for fixed jet-to-tube diameter ratio d/D that minimized the distance to mix as indicated by the color change of the indicator bromothymol blue. The same reaction was used to characterize other mixer geometries by Mao and Toor (1971), Pohorecki and Baldyga (1983), and Shenoy and Toor (1988). The assumption by Cozewith and Busko was that shorter distances for neutralization of the base correspond to improved tee-mixer performance. The latter circumstance would also mean greater entrainment rates of ambient HCl into the jet.

The optimum values corresponding to optimum tee design recorded by Cozewith and Busko are listed in Table 1. Since the acid-base reaction of Eq. 15 is instantaneous, the computed values of the Damkohler number are large or $10^4 < Da < 10^5$ that correspond to the mixing controlled limit.

Second moment

The optimum diameter ratios d/D and flow ratios $q/Q = (d/D)^2\ (u/v)$ are plotted in Figure 7 for the data of Tosun

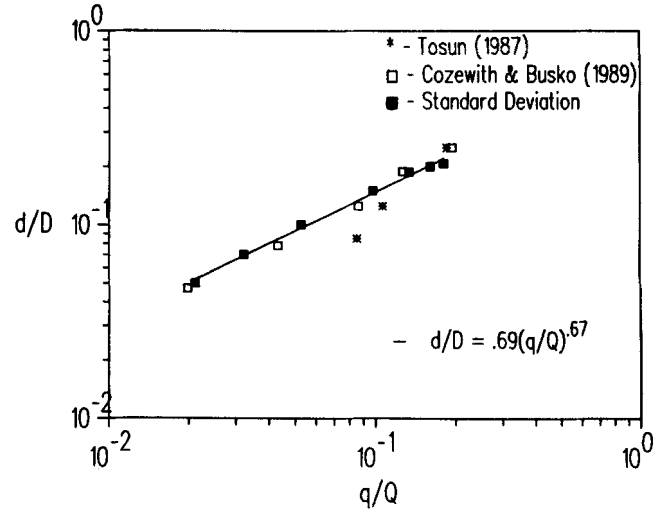

Figure 7. Optimum jet-to-tube diameter ratio vs. flow ratio from experiment (□) and numerical computation (■).

(1987) and Cozewith and Busko (1989) as tabulated in Table 1. The diameter and flow ratios corresponding to the local minimum in the relative standard deviation from numerical results similar to that plotted in Figure 6 are also shown in Figure 7. The numerical results clearly correlate the optimum geometry for the fast simple reaction of Cozewith and Busko in the mixing controlled limit where the optimum diameter ratio varies as the flow ratio to the 2/3 power. As expected, these results indicate that the dominate mechanism for optimum mixing is jet entrainment rather than wall impaction.

The three optimum data points of Tosun representing optimum selectivity (minimum X_s) are correlated with a maximum error of 30% and an average of 15%. With the limited number of data it is not clear whether these differences illustrate a diameter dependence on the Damkohler number, as suggested in Eq. 3, or experimental error. It should be noted that the two data points that deviate by 15% or more at smaller diameter and flow ratios correspond to $Da \cong 10^{-3}$, while the Damkohler number for the third point at $d/D = 0.25$ for the larger flow ratio is an order of magnitude larger, or $Da \cong 10^{-2}$. Again, jet entrainment appears to be the important mixing mechanism.

These results suggest that the scaling law of Eq. 3 for optimum mixing may be independent of the Damkohler number. One may conclude that the first reaction of Eq. 14 is fast (diffusion limited) or the optimum rate of mixing of A and B (maximize jet entrainment) would minimize the mean concentration of the reactants B and R in the rate expression for S. Moreover, the product of the turbulent reactant fluctuations $\overline{r'b'}$ of R and B in the rate expression for S may not depend on the Damkohler number as demonstrated by Toor (1969, 1975) for simple reactions.

Third moment

Numerical computations of the moment coefficient of skewness $m_3/m_2^{3/2}$, which is the third moment of the concentration distribution normalized with the standard deviation

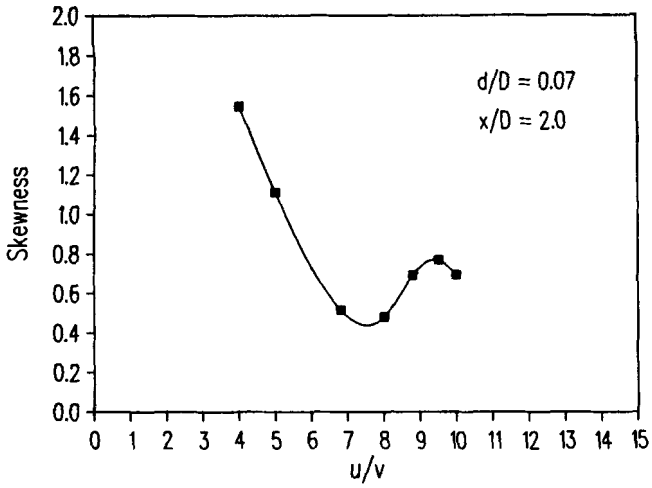

Figure 8. Moment coefficient of skewness $m_3/m_2^{3/2}$ vs. velocity ratio for fixed-tee geometry.

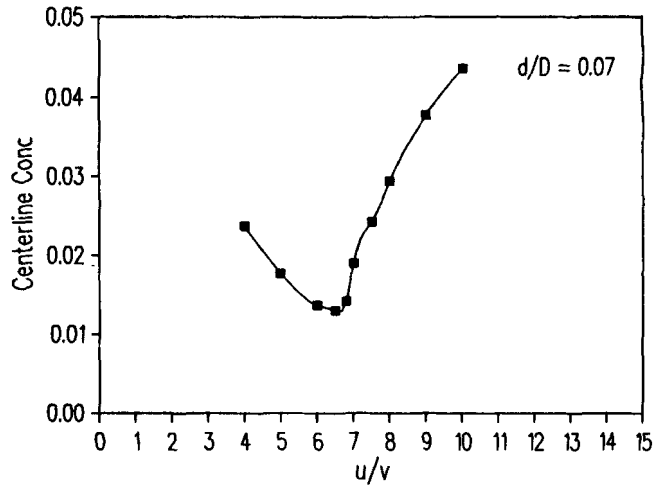

Figure 10. Maximum tracer concentration along opposite tube wall from jet inlet vs. jet-to-tube velocity ratio.

cubed, has been plotted on the ordinate of Figure 8 vs. jet-to-tube velocity ratio at fixed diameter ratio. As noted, there is a distinct minimum in the asymmetry of the concentration distribution at $u/v \cong 7.5$. These results are consistent with the picture of symmetry between the near and far wall of the tubular reactor at optimum conditions in the bottom contour of Figure 3.

Additional numerical results for a range of diameter ratios $0.05 \leq d/D \leq 0.25$ are plotted in Figure 9 and compared with the computed local minimum in the relative standard deviation previously illustrated in Figure 7. It is apparent from Figure 9 that symmetry and an entrainment-induced minimum in the relative standard deviation are synonymous.

Centerline concentration

Optimum jet entrainment prior to wall impaction should correspond with a reduction in the jet centerline concentration along the opposite wall of the tubular reactor. Figure 10 contains numerical computations of the centerline (maximum) tracer concentrations occurring along the opposite wall of the reactor for a range of jet-to-tube velocity ratios $4 \leq u/v \leq 10$ at fixed diameter ratio $d/D = 0.07$. It is evident from Figure 10 that $u/v \cong 6.5$ corresponds to a condition of maximum jet entrainment.

Additional optimum velocity ratios were computed for a range of diameter ratios $0.05 < d/D < 0.25$, and these results are compared in Figure 11 with previous calculations of the minimum in the relative standard deviation. Clearly, maximum jet entrainment is consistent with either a reduction in the scatter of the tracer concentration data or the degree of asymmetry in the concentration distribution.

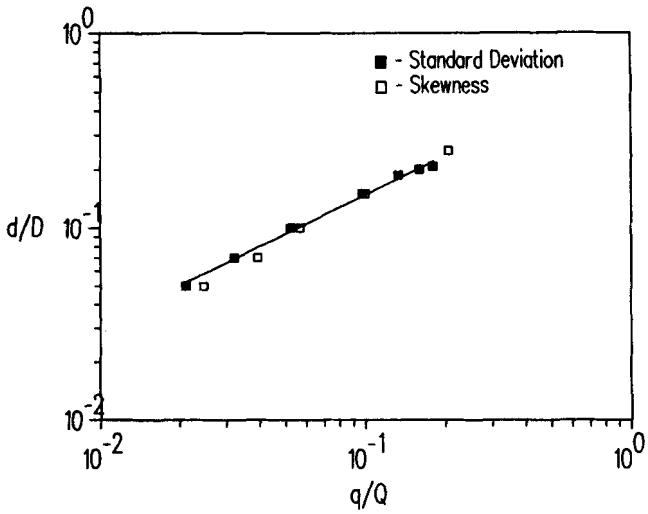

Figure 9. Optimum jet-to-tube diameter ratio vs. flow ratio.

Numerical computations of relative standard deviation (■) and moment coefficient of skewness (□) are compared.

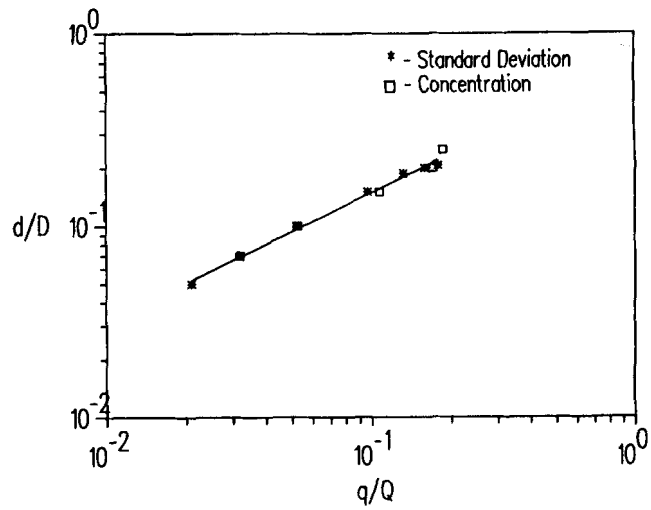

Figure 11. Optimum jet-to-tube diameter ratio vs. flow ratio.

Numerical computation of relative standard deviation (*) are compared with results from computations of jet centerline concentrations (□).

Geometric similarity

Considerable insight can be gained by analyzing the jet trajectory near the injection point for the simple geometry of Figure 1 (Forney and Kwon, 1979). Restricting the analysis to a right angle jet ($\theta_j = \pi/2$) and assuming uniform (top-hat) profiles for jet properties, one obtains an approximate jet trajectory valid for small departures from the origin $\theta \cong \pi/2$ and $x, z \cong 0$ (see Figure A1 in the Appendix):

$$\frac{z}{l_m} = \left(\frac{1/2}{\alpha + \beta/R}\right)^{1/2} \left(\frac{x}{l_m}\right)^{1/2}, \tag{16}$$

valid for $x/l_m < 1$, where the momentum length $l_m = d(u/v)$ and $R = u/v$.

Normalizing the coordinates x, z of Eq. 16 with respect to the tube diameter D, one obtains

$$\frac{z}{D} = \left(\frac{1/2}{\alpha + \beta/R}\right)^{1/2} \left(\frac{l_m}{D}\right)^{1/2} \left(\frac{x}{D}\right)^{1/2}. \tag{17}$$

One now assumes that optimum mixing is achieved when the jet impacts on the opposite tube wall at a fixed distance downstream from the injection point as shown in Figure 3. For simplicity, imposing the boundary conditions $z/D = 1.0$, $x/D = 0.5$, Eq. 17 becomes

$$\frac{l_m}{D} = 4\left(\alpha + \frac{\beta}{R}\right), \qquad R > 1, \tag{18}$$

where the entrainment parameters $\alpha = 0.11$ and $\beta = 0.6$ are universal constants (Hoult et al., 1969).

Since $q/Q = R(d/D)^2$, one obtains the optimum mixing ratio from Eq. 18

$$\frac{q}{Q} = 2\alpha\left(\frac{d}{D}\right)\left[1 + \left\{1 + \frac{\beta}{\alpha^2}\left(\frac{d}{D}\right)\right\}^{1/2}\right] \tag{19}$$

that provides the useful limits

$$\frac{d}{D} = \frac{1}{(4\beta)^{1/3}}(q/Q)^{2/3}, \qquad \frac{d}{D} \to 1$$

and

$$\frac{d}{D} = \frac{1}{(4\alpha)}(q/Q), \qquad \frac{d}{D} \to 0,$$

or substituting $\alpha = 0.11$ and $\beta = 0.6$, one obtains

$$\frac{d}{D} = 0.747(q/Q)^{2/3}, \qquad q/Q > 0.035 \tag{20}$$

and

$$\frac{d}{D} = 2.27(q/Q), \qquad q/Q < 0.035. \tag{21}$$

We note that Eq. 20 predicts the same 2/3 power law for the diameter and flow ratio dependence as that derived from the second-moment calculations plotted in Figure 7. Clearly, optimum jet entrainment, relative standard deviation, and skewness all represent geometrically similar flow fields in which the jet impacts against the opposite tube wall at a fixed number of tube diameters from the jet inlet. The scaling or similarity law is given by $d/D = 0.69\ (q/Q)^{2/3}$.

Acknowledgment

The first author (L. J. F.) wishes to acknowledge many helpful discussions with J. B. Gray and A. W. Etchells of DuPont and D. J. Koestler of Rohm & Haas. The financial support for the graduate study of Noureddine Nafia from Herschel Reese of Dow Corning is also gratefully acknowledged.

Notation

b_j = radius of jet, m
m_2 = second moment of tracer concentration
m_3 = third moment of tracer concentration
R = velocity ratio ($= u/v$)
v = mean upstream tube velocity, $m \cdot s^{-1}$
x, z = tube axial and radial distance from jet inlet, m
ρ = density, $kg \cdot m^3$
ν = kinematic viscosity, $m^2 \cdot s^{-1}$
θ = local angle between jet and tube axis

Literature Cited

Ajinkya, M. B., "Mixing of Gases," *Handbook of Fluids in Motion*, Chap. 9, N. P. Cheremisinoff and R. Gupta, eds., Ann Arbor Science Pub., Ann Arbor, MI (1983).

Baldyga, J., J. R. Bourne, B. Dubuis, A. W. Etchells, R. V. Cholap, and B. Zimmermann, "Jet Reactor Scale-Up for Mixing Controlled Reactions," *Trans. Inst. Chem. Eng.*, **73**, 497 (1995).

Baldyga, J., and J. R. Bourne, "Simplification of Micromixing Calculations—Part I: Derivation and Application of New Model," *Chem. Eng. J.*, **42**, 83 (1989).

Bourne, J. R., and S. Yu, "Investigation of Micromixing in Stirred Tank Reactors Using Parallel Reactions," *Ind. Eng. Chem. Res.*, **33**, 41 (1994).

Bourne, J. R., "Mixing in Single-Phase Chemical Reactors," *Mixing in the Process Industries*, Chap. 10, N. Harnby, M. Edwards, and A. Nienow, eds., Butterworth—Heinemann, Stoneham, MA, p. 184 (1992).

Bourne, J. R., F. Kozicki, and P. Rys, "Mixing and Fast Chemical Reaction: Test Reactions to Determine Segregation," *Chem. Eng. Sci.*, **36**, 1643 (1981).

Brodkey, R. S., ed., *Mixing in Turbulent Fields in Turbulence in Mixing Operations*, Academic Press, New York, p. 47 (1975).

Chilton, T. H., and R. P. Genereaux, "The Mixing of Gases for Reaction," *AIChE Trans.*, **25**, 103 (1930).

Cozewith, C., and M. Busko, "Design Correlations for Mixing Tees," *Ind. Eng. Chem. Res.*, **28**, 1521 (1989).

Cozewith, C., G. Ver Strate, T. J. Dalton, J. W. Frederick, and P. R. Ponzi, "Computer Simulation of Tee Mixers for Nonreactive and Reactive Flows," *Ind. Eng. Chem. Res.*, **30**, 270 (1991).

Fay, J. A., "Buoyant Plumes and Wakes," *Annu. Rev. Fluid Mech.*, **5**, 151 (1973).

Fitzgerald, S. D., and E. R. Holley, "Jet Injections for Optimum Mixing in Pipe Flow," *J. Hydraul. Div., Am. Soc. Civ. Eng.*, **107**(HY 10), 1179 (1981).

Forney, L. J., and T. C. Kwon, "Efficient Single Jet Mixing in Turbulent Tube Flow," *AIChE J.*, **25**, 623 (1979).

Forney, L. J., and H. C. Lee, "Optimum Dimensions for Pipeline Mixing at a T-Junction," *AIChE J.*, **28**, 980 (1982).

Forney, L. J., "Jet Injection for Optimum Pipeline Mixing," *Encyclopedia of Fluid Mechanics*, Vol. II, Chap. 25, N. P. Cheremisinoff, ed., Gulf Pub., Houston (1986).
Forney, L. J., and G. E. Gray, "Optimum Design of a Tee Mixer for Fast Reactions," *AIChE J.*, **36**, 1773 (1990).
Ger, A. M., and E. R. Holley, "Comparison of Single-Point Injections in Pipe Flow," *J. Hydraul. Div., Am. Soc. Civ. Eng.*, **102**(HY6), 731 (1976).
Gosman, A. D., and R. Simitovic, "An Experiment Study of Confined Jet Mixing," *Chem. Eng. Sci.*, **41**, 1953 (1986).
Gray, J. B., "Turbulent Radial Mixing in Pipes," *Mixing: Theory and Practice*, Vol. III, Chap. 13, J. B. Gray and V. W. Uhl, eds., Academic Press, New York (1986).
Hoult, D. P., J. A. Fay, and L. J. Forney, "A Theory of Plume Rise Compared with Field Observations," *J. Air Pollut. Contr. Assoc.*, **19**, 585 (1969).
Mao, K. W., and H. L. Toor, "Second Order Chemical Reactions with Turbulent Mixing," *Ind. Eng. Chem. Fundam.*, **10**, 192 (1971).
Maruyama, T., S. Suzuki, and T. Mizushina, "Pipeline Mixing Between Two Fluid Streams Meeting at a T-Junction," *Int. Chem. Eng.*, **21**, 205 (1981).
Maruyama, T., T. Mizushina, and F. Watanabe, "Turbulent Mixing of Two Fluid Streams at an Oblique Branch," *Int. Chem. Eng.*, **22**, 287 (1982).
Maruyama, T., T. Mizushina, and S. Hayashiguchi, "Optimum Jet Mixing in Turbulent Pipe Flow," *Int. Chem. Eng.*, **23**, 707 (1983).
Monclova, L. A., and L. J. Forney, "Numerical Simulation of Pipeline Tee Mixers," *Ind. Eng. Chem. Res.*, **34**, 1488 (1995).
Morton, B. R., G. I. Taylor, and J. S. Turner, "Turbulent Gravitational Convection from Maintained and Instantaneous Sources," *Proc. Roy. Soc. London A*, **234**, 1 (1956).
Narayan, B. C., "Experimental Study of the Rates of Turbulent Mixing in Pipe Flow," MS Thesis, Univ. of Tulsa, Tulsa, OK (1971).
O'Leary, C. D., and L. J. Forney, "Optimization of In-Line Mixing at a 90 Tee," *Ind. Eng. Chem. Process Des. Dev.*, **24**, 332 (1985).
Patterson, G., *Simulating Turbulent-Field Mixers and Reactors -or- Taking the Art of the Design in Turbulence in Mixing Operations*, R. S. Brodkey, ed., Academic Press, New York, p. 221 (1975).
Pohorecki, R., and J. Baldyga, "New Model of Micromixing in Chemical Reactors," *Ind. Eng. Chem. Fund.*, **22**, 392 (1983).
Reed, R. D., and B. C. Narayan, "Mixing Fluids Under Turbulent Flow Conditions," *Chem. Eng.*, **86**, 131 (1979).
Shenoy, U. V., and H. L. Toor, "Micromixing Measurements with Chemical Indicators," AIChE Meeting, Washington, DC (1988).
Simpson, L. L., "Turbulence and Industrial Mixing," *Chem. Eng. Prog.*, **70**, 77 (1974).
Sroka, L. M., and L. J. Forney, "Fluid Mixing with a Pipeline Tee: Theory and Experiment," *AIChE J.*, **35**, 406 (1989).
Toor, H. L., "Turbulent Mixing of Two Species with and without Chemical Reactions," *Ind. Eng. Chem. Fundam.*, **8**, 655 (1969).
Toor, H. L., *The Non-premixed Reactions $A + B \rightarrow$ Products in Turbulence in Mixing Operations*, R. S. Brodkey, ed., Academic Press, New York, p. 121 (1975).
Tosun, G. A., "A Study of Micromixing in Tee Mixers," *Ind. Eng. Chem. Res.*, **26**, 1184 (1987).
Ver Strate, G., C. Cozewith, and S. Ju, "Near Monodisperse Ethylene–Propylene Copolymers by Direct Ziegler–Natta Polymerization," *Macromol.*, **21**, 3360 (1988).

Appendix 1: Entrainment rates: Right angle or coaxial

The two simple ways of mixing reactants in a tube are right-angle jet injection, as considered in the present article (see Figure 1) or a coaxial jet with one reactant introduced into the reactor with a small tube parallel to a larger diameter tube axis (see Figure A1). Since turbulent jets entrain ambient fluid, the rate of mixing is determined by the jet entrainment rate. In the case of right-angle injection, the entrainment rate also determines the jet trajectory in the reactor tube.

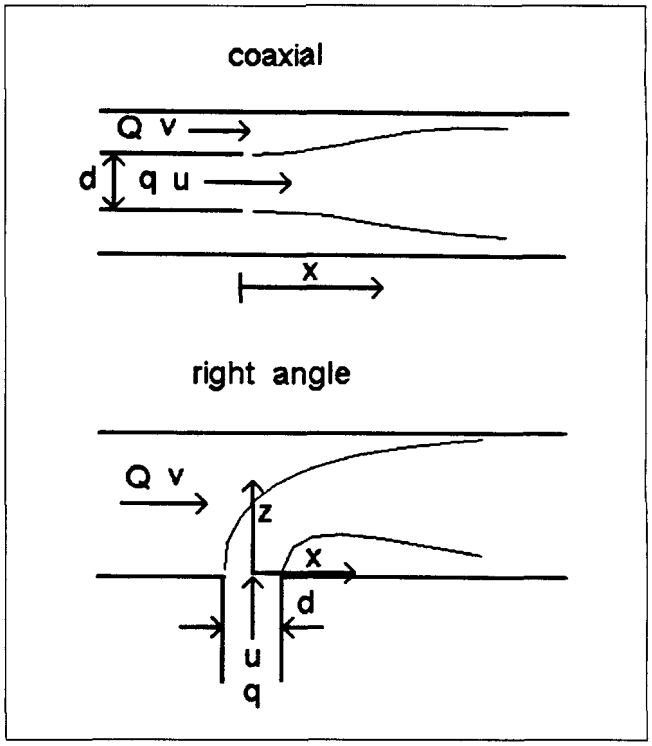

Figure A1. Coaxial and right-angle jet injection.

We assume that there are two additive entrainment mechanisms: one is due to the tangential difference between the local jet velocity u and ambient fluid velocity component parallel to the jet and the other to the ambient fluid velocity normal to the jet (Morton et al., 1956; Hoult et al., 1969; Fay, 1973). It is also assumed that the rate of entrainment for each mechanism is the product of a nondimensional entrainment parameter (α or β independent of position) and the product of the jet perimeter and the corresponding velocity differences.

For simplicity, the circular jet velocity profile is assumed to have the shape of a top hat, and we neglect density differences between the jet and ambient fluid. Thus, we obtain expressions for the rate of entrainment of ambient fluid at the jet inlet x, $z \cong 0$ for both geometries in the form

right angle:

$$\frac{d}{dz}(\pi b^2 u) = 2\pi b_j(\alpha u_j + \beta v) \tag{A1}$$

coaxial:

$$\frac{d}{dx}(\pi b^2 u) = 2\pi b_j \alpha(u_j - v), \tag{A2}$$

where $\alpha = 0.11$ is the tangential entrainment parameter and $\beta = 0.6$ is the normal entrainment parameter. The coordinates x, z are measured from the jet inlet parallel to the reactor axis or along its diameter, respectively, as shown in Figure A1.

Therefore, the ratio of right angle to coaxial entrainment rates at the jet inlet becomes

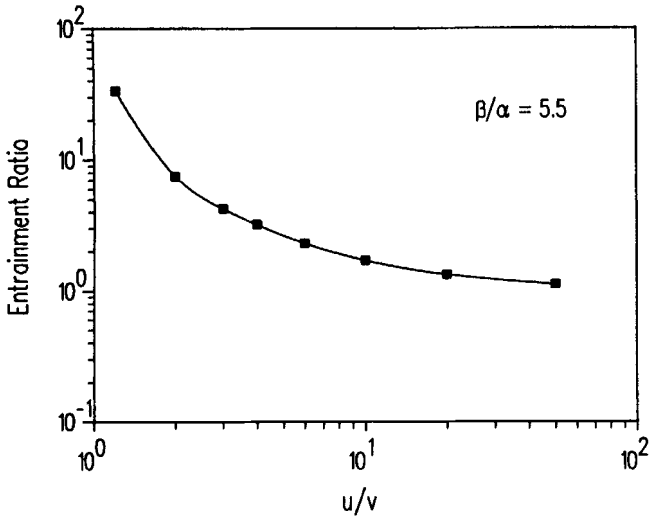

Figure A2. Ratio of right-angle-to-coaxial entrainment rate at the jet inlet vs. jet-to-tube velocity ratio.

Jet diameter is the same for both geometries.

$$\frac{d}{dz}(\pi b^2 u)/\frac{d}{dx}(\pi b^2 u) = \frac{u/v + \beta/2}{u/v - 1}. \qquad \text{(A3)}$$

Assuming that the jet diameter $d = 2b_j$ and flow rates u in both jets are equal and that the ambient fluid velocity v is identical where $u > v$, it is clearly desirable to use right-angle jets as shown in Figure A1 to take advantage of the large normal entrainment mechanism. Noting that $u/v > 1$ and $\beta/\alpha = 5.5$, the ratio of entrainment rates is shown in Figure A2.

Appendix 2: Mixing time

The jet Reynolds number represents the ratio of inertial forces ρu^2 to viscous forces $\mu u/d$ or $Re_j = \rho ud/\mu$. If $Re_j \geq 10^4$, the fluid viscosity is not important and the only way to form a time scale for mixing is the ratio of velocity-to-diameter or $t_{mix} \alpha\ d/u$. The same result could be derived by starting with the integral length scale for the jet $l \cong d$ and the energy dissipation rate $\epsilon \cong u^3/d$ (e.g., Baldyga et al., 1995).

Manuscript received Jan. 26, 1996, and revision received Apr. 8, 1996.